EARTH SURFACE PROCESSES AND LANDFORMS
Earth Surf. Process. Landforms (2017)

Published online in Wiley Online Library
(wileyonlinelibrary.com) DOI: 10.1002/esp.4099

Late quaternary speleogenesis and landscape evolution in the northern Apennine evaporite areas

Andrea Columbu,[1]* Veronica Chiarini,[2,3] Jo De Waele,[2] Russell Drysdale,[1,3] Jon Woodhead,[4] John Hellstrom[4] and Paolo Forti[2]
[1] School of Geography, University of Melbourne, 221 Bouverie Street, 3010 Melbourne, Australia
[2] Department of Biological, Geological and Environmental Sciences, University of Bologna, Via Zamboni 67, 40127 Bologna, Italy
[3] Laboratoire EDYTEM, University of Savoie, bd de la Mer Caspienne, Le Bourget du Lac cedex F-73376, France
[4] School of Earth Sciences, University of Melbourne, Corner Swanston & Elgin Streets, 3010 Melbourne, Australia

Received 9 June 2016; Revised 7 December 2016; Accepted 8 December 2016

*Correspondence to: Andrea Columbu, School of Geography, University of Melbourne, 221 Bouverie Street, 3010, Melbourne, Australia. E-mail: acolumbu@student.unimelb.edu.au

ESPL
Earth Surface Processes and Landforms

ABSTRACT: Gypsum beds host the majority of the caves in the north-eastern flank of the Apennines, in the Emilia Romagna region (Italy). More than six hundred of these caves have been surveyed, including the longest known epigenic gypsum cave systems in the world (Spipola-Acquafredda, ~11 km). Although this area has been intensively studied from a geological point of view, the age of the caves has never been investigated in detail. The rapid dissolution of gypsum and uplift history of the area have led to the long-held view that speleogenesis commenced only during the last 130 000 years.

Epigenic caves only form when the surface drainage system efficiently conveys water into the underground. In the study area, this was achieved after the dismantling of most of the impervious sediments covering the gypsum and the development of protovalleys and sinkholes. The time necessary for these processes can by constrained by understanding when caves were first formed.

The minimum age of karst voids can be indirectly estimated by dating the infilling sediments. U–Th dating of carbonate speleothems growing in gypsum caves has been applied to 20 samples from 14 different caves from the Spipola-Acquafredda, Monte Tondo-Re Tiberio, Stella-Rio Basino, Monte Mauro, and Castelnuovo systems. The results show that: (i) caves have been forming since at least ~600 kyr ago; (ii) the peak of speleogenesis was reached during relatively cold climate stages, when rivers formed terraces at the surface and aggradation caused paragenesis in the stable cave levels; (iii) ~200 000 years were necessary for the dismantling of most of the sediments covering the karstifiable gypsum and the development of a surface mature drainage network.

Besides providing a significant contribution to the understanding of evaporite karst evolution in the Apennines, this study refines our knowledge on the timescale of geomorphological processes in a region affected by rapid uplifting. Copyright © 2016 John Wiley & Sons, Ltd.

KEYWORDS: carbonate speleothems; evaporite karst; landscape evolution; cave formation; palaeoclimate

Introduction

Caves can form under two main hydrochemical conditions: epigenic and hypogenic (Klimchouk, 2007). Surface waters that derive their aggressiveness from the land surface and the atmosphere carve epigenic caves, while fluids attaining their acidity from deep sources (i.e. rising H_2S or CO_2, or mixing of two different solutions such as in coastal settings) are responsible for the formation of hypogenic caves. Hypogenic speleogenesis, often happening deep below the Earth surface, can act over very long time spans (Polyak *et al.*, 1998). Epigenic speleogenesis, on the other hand, occurs closer to the land surface, and erosional processes tend to intercept karst voids in a few millions of years.

Karst dynamics are intimately associated with environmental variations at the surface (Ford and Williams, 2007), and the chronological refinement of dissolution processes and karst history may help us to better understand base-level (i.e. local water table) variation, which is related to geological events such as uplift and other tectonic movements, as well as valley incision. In this regard, the study of epigenic caves carved in gypsum provides some advantages compared with those hosted in limestone/dolostone. Gypsum is highly soluble, and speleogenesis occurs up to 100 times faster than in carbonates (Klimchouk, 2000). The explorable caves at present, if not confined in deeper levels of the geological sequence (i.e. hypogenic Ukrainian systems, Klimchouk, 2012), must be relatively young because the rapid underground erosion combined with surface weathering lead inevitably to the fast dismantling of the bedrock, demolishing the underlying caves. On the other hand, high gypsum solubility provides an almost contemporaneous response of speleogenesis to surface climatic and environmental changes, even at intra-Milankovitch time-scales (Columbu *et al.*, 2015). It follows that dating epigenic gypsum caves offers the double opportunity of constraining the timing of cave formation and allowing a better understanding of the link between external and underground geological processes. Consequently, because of the link between epigenic caves and surface realms, understanding the age of the first proto-caves provides important insights to the timing of geomorphological evolution at the surface. Specifically, it constrains the time necessary for: (1) the exhumation of the karst terrain (i.e. when karstifiable bedrock is no longer confined and starts to undergo surface weathering and erosion); and (ii) the development of surface drainage capable of efficiently conveying water into the subterraneous system, thus forming epigenic caves (i.e. formation of protovalleys, sinkholes, and dolines).

One of the most intriguing – yet complicated – conundrums when studying the genesis and evolution of cave systems is an understanding of the exact timing of void formation, i.e. the problem of assigning a numeric age to 'what is not there' (Sasowsky, 1998); a range of strategies have been proposed in order to overcome this problem. The ages obtained by the dating of alunite in Carlsbad and Lechuguilla caves are considered contemporaneous with the formation of the cave passages (Polyak *et al.*, 1998), because this mineral forms when the acidic cave-forming waters encounter clays. In the same area, dolomite has also been reported as a speleogenetic byproduct (Polyak *et al.*, 2016) Similarly, replacement gypsum in sulphuric-acid caves can provide reliable ages of cave formation, as long as gypsum did not undergo alteration – and did not loose uranium – over time (Plan *et al.*, 2012; Piccini *et al.*, 2015). These can be considered the nearest direct approaches to dating a void. However, the survival of alunite and/or gypsum is restricted to those parts of the cave that have never experienced flooding, dripping or seepage since their formation. In addition, formation of speleogenetic dolomite is possible in restricted circumstances. Also, these minerals are only found in sulphuric-acid caves, strongly limiting the utilisation of this direct-dating approach. As a result, karst voids are mostly indirectly dated (Audra *et al.*, 2006) using a range of infilling materials that logically are formed subsequent to the carving of the cave. These materials include sediments, archaeological remains, fossils and speleothems.

The speleogenesis of epigenic limestone and dolostone karst systems is often driven by changes of the local base-level at the surface (Williams, 1982; Ford and Williams, 2007). This means that bedrock exhumation, allowing the start of speleogenesis, may have happened many millions of years ago. In addition, with the exception of tropical environments (Farrant *et al.*, 1995; Audra *et al.*, 2011), cave development in carbonate rocks is a slow process (White, 1988). It follows that the formation of those karst networks currently showing complex multi-kilometric extensions may have begun several millions of years before present (De Waele *et al.*, 2012a; Tassy *et al.*, 2013; Calvet *et al.*, 2015; Häuselmann *et al.*, 2015). In such cases the datable materials traceable to the first stages of cave evolution may have been irretrievably lost, and even the primordial asset of the karst passages is probably overwritten by more recent speleogenetic phenomena. For example, dated speleothems from the middle levels (~900 m a.s.l.) of the Corchia system (central Italy) approach one million years in age (Woodhead *et al.*, 2006; Bajo *et al.*, 2012), while the exhumation of the area occurred not earlier than 5.0–4.5 Ma ago (Balestrieri *et al.*, 2003). The formation of the earliest upper levels (~1400 m a.s.l.) is assigned to the Late Pliocene (Piccini, 2011), and further U/Pb dating of speleothems from the highest cave levels would be needed to refine this chronological constraint.

We studied several still-active karst systems carved in the gypsum sequence outcropping in the Northern Apennine foothills, Emilia Romagna region, Italy (De Waele *et al.*, 2011). Earlier studies have also reported Late Messinian karst systems in this area, now entirely filled with sediments. These 5 million year old cave segments formed before the gypsum sequence was covered with the thick, less permeable, Argille Azzurre Fm. and tilted in its actual monocline position (De Waele and Pasini, 2013). Epigenic caves in gypsum could not have formed since the Late Messinian submersion, and the most recent karst cycle started only after the Apennines emerged from the sea and most of the covering sediments were removed from the gypsum sequence. In this portion of the Apennine piedmont, karst networks are mostly composed of superimposed, more or less horizontal, tunnels that reflect the position of past local base levels (Columbu *et al.*, 2015). We integrated the U–Th dating of twenty carbonate speleothems, which provide minimum ages of the passages in which they grew, with in-cave and external morphological features that are indicators of the palaeo base levels. These data have then been combined with regional geological relationships to document the Quaternary evolution of the underground and surface drainage of the area of study. The main aims and motivations of the paper therefore are:

(1) To establish the timing of the inception of speleogenesis. For the aforementioned reasons the ages of these caves have been largely underestimated in the past. Previous research has linked the speleogenesis to the last 130 000 years (Demaria, 2002; Forti, 2003; Pasini, 2012); limited radiometric ages (Forti and Chiesi, 2001; Forti, 2003), and archaeological (Miari, 2007; Negrini, 2007) and paleontological (Pasini, 1969) findings have corroborated this idea.
(2) To understand the periods during which the excavation of the different cave levels constituting the systems was most effective.
(3) To evaluate the time necessary for the dismantling of impervious rocks originally covering the karstifiable gypsum unit and for the excavation of the first valleys, dolines and sinkholes, which allowed the penetration of water into the epigenic karst network.

Considering the above-said link between the subterranean and surface environments, the outcomes may reinforce our knowledge of the connection between the rapid uplift that is characteristic of the study area (Cyr and Granger, 2008; Picotti and Pazzaglia, 2008) and the landscape evolution of the middle to upper Pleistocene.

Study area

We explored five karst systems located in the northern Apennine piedmont (Emilia-Romagna region), carved in the *Vena del Gesso* (= Gypsum vein) formation (Vai and Martini, 2001; Lugli *et al.*, 2010): Spipola-Acquafredda, Monte Tondo-Re Tiberio, Stella-Rio Basino, Monte Mauro and Castelnuovo (Figure 1). The first lies at the south-eastern periphery of Bologna (Figure 2(A)), while the remaining caves are situated ~40 km south-east of the city (south of the city of Imola), where the gypsum vein outcrops with its classical cuesta-like morphology (Figure 2(B)). The gypsum vein is mostly composed of macrocrystallyne selenitic gypsum. In macrocrystalline gypsum, pervasive primary porosity is scarce. Superficial water infiltrates into the underground once the bedrock is exposed by vadose fractures and joints originated

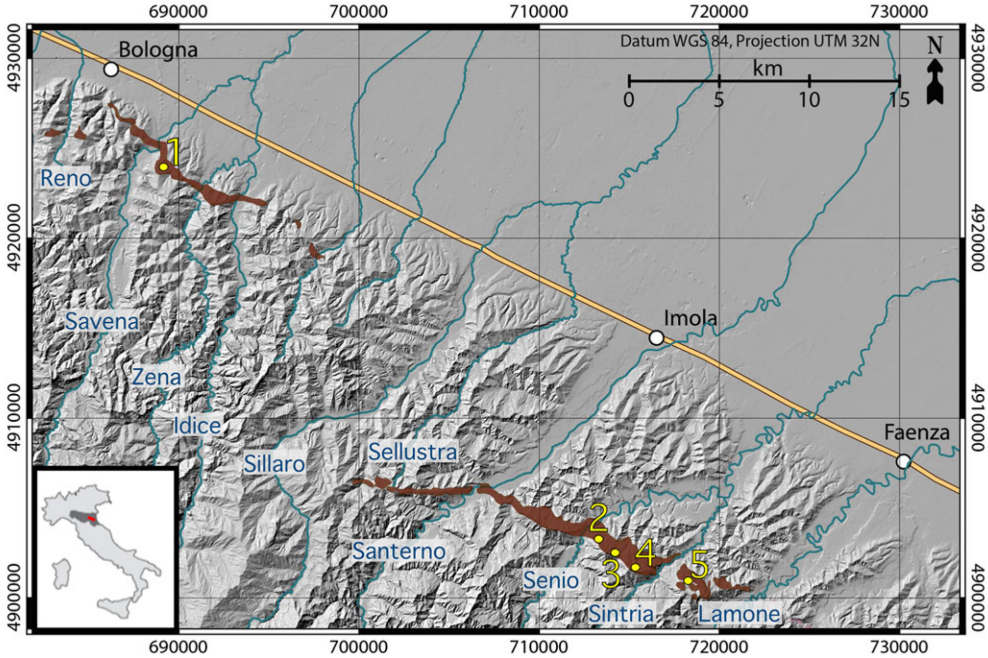

Figure 1. The study area. The inset shows the Emilia-Romagna region (dark grey) and the cave site (red rectangle). The main map shows the outcropping gypsum ridge (brown shading); the main karst systems are shown with circles and numbers (1 = Spipola–Acquafredda, 2 = Monte Tondo–Re Tiberio, 3 = Stella–Rio Basino, 4 = Monte Mauro, 5 = Castelnuovo). The names of the rivers draining this portion of the Apennines are shown in blue; most of them constitute the local base level for the studied karst systems. The straight line is the A1 highway, which roughly follows the boundary between the Apennine foothills to the south and the Po Plain to the north. [Colour figure can be viewed at wileyonlinelibrary.com]

by tectonic and/or diagenesis. Superficial karst landforms are also well developed in the study area (i.e. dolines and blind valleys, Figure 2), having a primary role in the current and past development of the underground drainage network. Gypsum in the Italian peninsula, excluding the few Permian and Triassic outcrops, was deposited during the Messinian Salinity crisis (Krijgsman *et al.*, 1999; Roveri *et al.*, 2014). In the Northern Apennines, it is exposed along a NW–SE elongated belt connecting the peaks of the mountain chain in the south with the Po plain foredeep in the north (Figure 1). The structure of the caves comprising the explored karst systems is intimately related to the geological and environmental factors that have characterised the area since the uplift of the Apennines. First, the majority of caves follow NW–SE tectonic features (De Waele and Piccini, 2008); less frequently WNW–ESE and W–E lineaments, or the SW–NE anti-Apennine directions, are exploited. Second, all caverns are epigenic (Klimchouk, 2000), developed in an unconfined aquifer in the first few hundred metres of the exposed bedrock. Considering that the karst conduits convey the infiltrating waters to the local base level, the altitude and elongation of the caves is related to base-level oscillations over time, associated with Quaternary climate changes and uplift (Columbu *et al.*, 2015). Several superimposed levels constitute the Spipola-Acquafredda and Monte Tondo systems, of which only the lowermost is currently active. Two levels form the Castelnuovo system and the Stella-Basino system, possibly reflecting the younger age of these two networks (Chiarini *et al.*, 2015). At Monte Mauro, on the other hand, the Grotta dei Banditi (Bandit cave) is the only branch left of a much bigger cave system, now completely eroded. Remains of carbonate flowstones that can still be found at the surface close to Grotta dei Banditi are all that is left of the other branches of this system. In fact, any review of the gypsum caves in the Emilia-Romagna territories should also consider those caves that are no longer visible today, destroyed by the continuous surface and subterranean erosion of the soft gypsum beds.

Materials and methods

In order to promote cave conservation (Fairchild and Baker, 2012; Scroxton *et al.*, 2016), no *in situ* carbonate speleothems were removed; samples were principally found as broken specimens inside the caves. In a few cases, speleothems were subjected to core drilling (Spötl and Mattey, 2012; Figure 2(C)) or found at the surface, in the vicinity of the cave entrance. Six flowstones were collected at the Monte Tondo-Re Tiberio system (RTf, A50, 3A, RTy, PP and GO) (Figure 2(E)). The first was found in the quarry at ~340 m a.s.l., while the remaining samples were collected in cave galleries, respectively, at 270, 220, 180, 160 and 130 metres a.s.l. Two flowstones and one stalagmite were sampled in both the Spipola-Acquafredda and Castelnuovo karst systems. In the first, the SpD flowstone was found at the Croara quarry (250 metres a.s.l.) close to the Spipola doline (Figure 2(E)) (Forti and Sauro, 1996), the Sp1 flowstone cored in a cave level at 120 m a.s.l. (Figure 2(D)) and SpS found in a cave level at 125 m a.s.l. In Castelnuovo, the Mor2 stalagmite was found in the Mornig cave at 190 m a.s.l, the P2 flowstone was recovered at the surface at 180 m a.s.l and the P3 flowstone was cored in a cave level at 185 m a.s.l. The exploration of the Monte Mauro cave system allowed us to recover a large stalagmite (BA_Big) from Banditi Cave at 450 m a.s.l., and two flowstones (Ba1 and Ba2) near the cave but at the surface (unroofed remains of a larger cave system). Two other flowstones (MM4 and MM2) were taken at the surface close to the highest elevation of Monte Mauro, around 480–490 m a.s.l. Three flowstones also come from the Stella-Rio Basino system: RBT was found at the surface at 160 m a.s.l, RB1 and RB3 were collected underground at 170 m a.s.l. The predominance of flowstones over stalagmites is not a sampling bias: stalagmites are generally extremely rare in the Northern Apennine gypsum karst. Refer to Figure 3 for the size and macroscopic fabric of the samples.

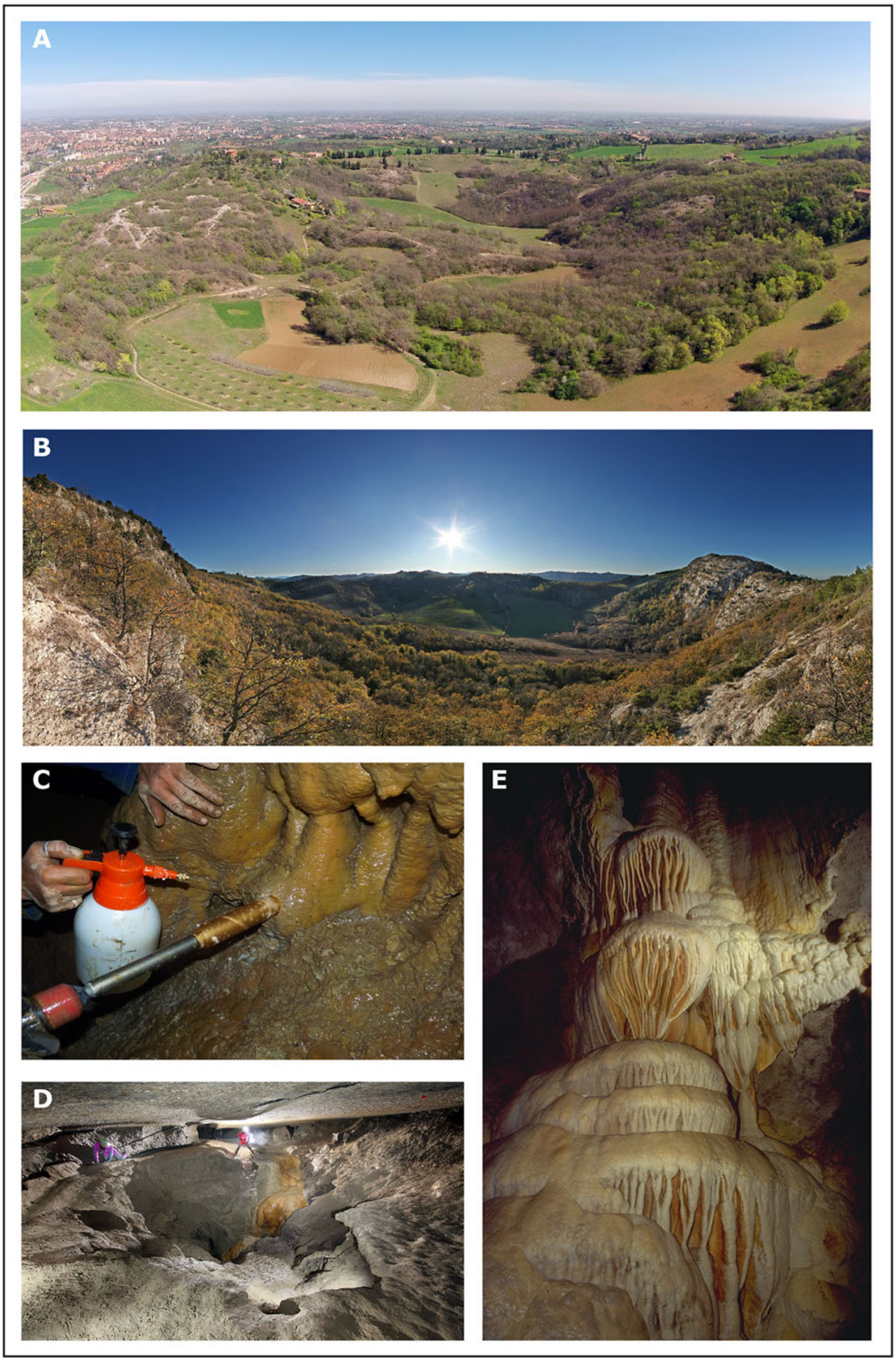

Figure 2. Gypsum karst superficial and subterranean landforms. (A) Spipola doline in the gypsum area on the outskirts of Bologna (the city centre can be seen in the left background): the cave entrance is located at the base of the doline (photo Francesco Grazioli). (B) The Vena del Gesso gypsum ridge (right) forming a characteristic cuesta-like landscape. At its base the Rio Stella River sinks forming the Stella–Rio Basino through the cave (photo Piero Lucci). (C) Drilling a flowstone in the Tanaccia cave (Castelnuovo karst system), Vena del Gesso (photo Veronica Chiarini). (D) The still active flowstone in the Spipola cave, Bologna (Photo Francesco Grazioli). (E) The Pozzo Pollini flowstone in the Re Tiberio cave system, intercepted by the underground gypsum quarry (Photo Claudio Pollini). [Colour figure can be viewed at wileyonlinelibrary.com]

The speleothems were sliced in two with a diamond saw. The analyses were performed on the fresh surface of one half after polishing; the other half was archived. The sub-samples (calcite prisms) used for the U–Th dating weighed between 10 and 120 mg, and were drilled along the growth layers using a dental hand-drill. The dating aimed to recover the base and top age of all the speleothems. When the stratigraphic bottom/top was considered unsuitable for dating (i.e. due to the visible presence of detrital material in the carbonate layers, evidence of carbonate dissolution, etc.), samples were taken of the closest clean and unaltered calcite. Intermediate ages were also determined in order to improve the chronological control of the longest samples.

In total, 70 U–Th ages were produced. The sub-samples, the drilling locations of which are reported in Figure 3, were first dissolved in HNO_3 following the procedure of Hellstrom (2003). A spike of known $^{236}U/^{233}U/^{229}Th$ ratio was added to the solution and the U–Th fraction was separated from the

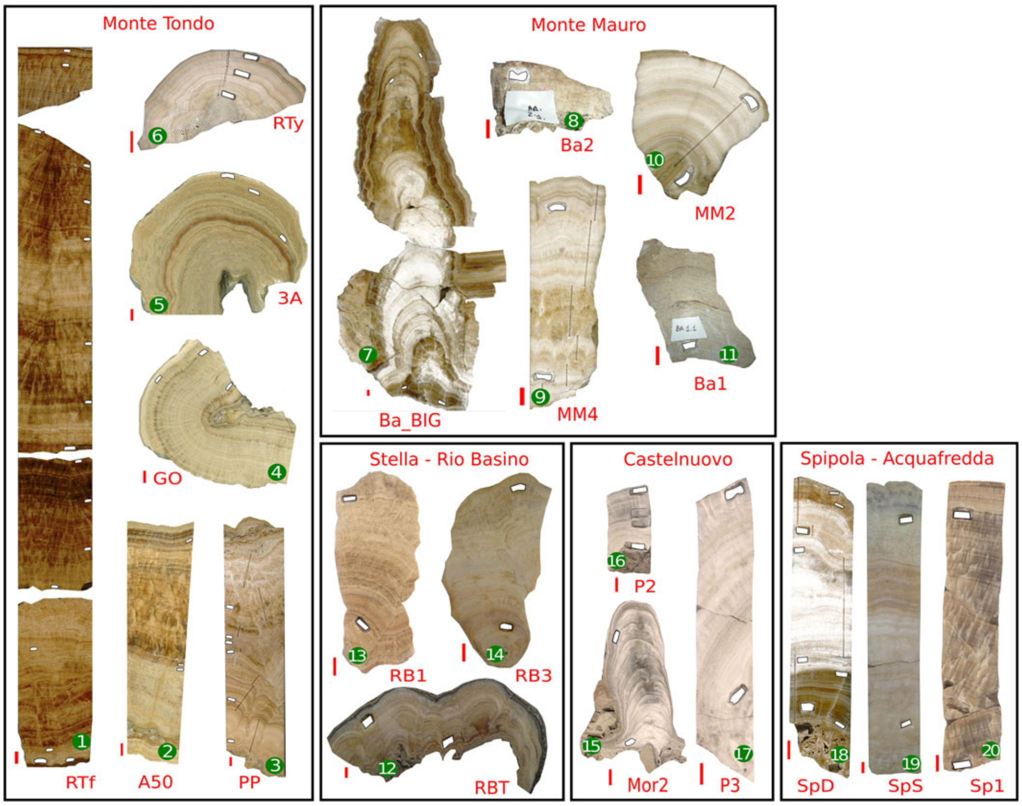

Figure 3. Speleothems used in this study. The white boxes indicate the locations of the samples extracted for the U–Th radiometric dating. The red bar is 1 cm long. The white numbers are used as a reference in Figure 7. [Colour figure can be viewed at wileyonlinelibrary.com]

carbonate matrix using Eichrom TRU-Spec resin in columns. The U and Th fractions were collected together and evaporated overnight at 80°C before being taken up in 5% HNO3/0.5% HF ready for isotopic analysis. The majority of measurements were performed on a Nu Plasma multi-collector–inductively coupled plasma–mass spectrometer (MC-ICP-MS) at the School of Earth Sciences, The University of Melbourne, following the methodology established in Hellstrom (2003) and refined in Drysdale *et al.* (2012). Three samples were analysed instead at the Laboratoire des Sciences du Climat et de l'Environnement (LSCE) at Gif-sur-Yvette (France) following Pons-Branchu *et al.* (2014) (Table I). Th-corrected U–Th ages were calculated using Equation (1) of Hellstrom (2006) with the ^{230}Th–^{234}U decay constants of Cheng *et al.* (2013) and an initial (^{230}Th/^{232}Th)$_i$ of 1.5 ± 1.5. Samples were analysed in batches of 24 with 8 accompanying HU-1 Harwell Uraninite measurements, and reported activity ratio uncertainties are expanded by the observed standard deviations of the standards. Age uncertainties are approximated as symmetric, except for the oldest samples where separate upper and lower uncertainty bounds were calculated.

Results

In general, the speleothem ages produced realistic radiometric ages, with samples possessing a high content of ^{238}U and, for the most part, a high $^{230/232}$Th activity ratio (^{230}Th/^{232}Th; Table I). ^{238}U is never below 290 ng g^{-1}, with maximum concentrations exceeding 3000 ng g^{-1}, and with an average value of 1206 ng g^{-1}. (^{230}Th/^{232}Th) averages ~8000, but it correlates with the age of the speleothems. The Holocene samples report the lowest values (<10), followed by speleothems deposited during the early last glacial (100–200). In older samples (i.e. last interglacial or older) this ratio is two to three orders of magnitude greater. Initial ^{232}Th content has an important role in determining the 2σ uncertainty associated with the final age. Young samples possess relatively small amounts of authigenic ^{230}Th, thus (^{230}Th/^{232}Th) and corrected age uncertainty are highly sensitive to thorium derived from non-authigenic sources. For this reason, the uncertainties relative to the Holocene ages are, in percentage terms, greater than the other samples.

The final corrected ages and the associated errors are reported in Table I. A comparison of speleothem age with the main climatic stages over the last ~800 ka is provided in Figure 4. The compilation follows the subdivision of the marine isotopic stages (MIS; Emiliani, 1955) on the global 'LR04' δ^{18}O benthic stack proposed by Lisiecki and Raymo (2005). Four speleothems grew during the last two millennia of the Holocene (MIS1) (RTy, Sp1, SpS, and RB3) while seven speleothems span from the middle (Mor2, RB1, RBT, and P3) to the early Holocene (GO and P2). Flowstones 3A, PP, and A50 were deposited during shorts intervals of the period ranging from ~110 ka to ~70 ka, the transitional phase from the last interglacial (MIS 5e) to the last glacial, characterised by the Greenland Interstadial (GI) and Stadial (GS) oscillation (NGRIP project members, 2004). Speleothem 3A formed from 108.86 ± 0.98 to 106.29 ± 7.23 ka, PP from 87.80 ± 0.70 to 75.21 ± 1.44 ka and A50 from 77.89 ± 6.06 to 74.69 ± 0.68 ka, correlated, respectively, with GI 24 and 21–20 (Columbu *et al.*, 2015). Two speleothems formed during the last interglacial: RTf and Ba_Big. They were mainly deposited during the climatic climax (~130–120 ka, MIS 5e), although the upper portion of the Ba_Big stalagmite grew across the LIG-glacial transition (top age 112.36 ± 1.09 ka). Flowstone SpD started to grow during the last phase of the glaciation corresponding to the MIS 8, but was mostly formed during the MIS 7e, from 253.90 ± 4.41 to 239.34 ± 4.30 ka. Two flowstones from the Monte Mauro system, MM4 and MM2, reported bottom ages much older than the top ages. MM4 bottom is at 468.00 $^{+130}/_{-42}$ ka (MIS 13 considering the

Table I. U-Th radiometric dating results. Mass of samples, 238U content, the uranium and thorium isotope activity ratios, and the uncorrected and corrected ages are provided. Uncertainties are expressed in 2σ notation. Ages are calculated using equation 1 of Hellstrom (2006) and the U and Th decay constants of Cheng *et al.* (2013). The raw ages were corrected using an initial 230/232Th activity ratio of 1.5 ± 1.5. All the analyses were performed at the School of Earth Science, University of Melbourne; except D2, D3 and D4 (Pozzo Pollini) subsamples, which were instead analysed at LSCE (Columbu *et al.*, 2015)

Cave system	Cave	Sample ID	Mass (g)	^{238}U (ng/g)	($^{230}Th/^{238}U$)A	2σ	($^{234}U/^{238}U$)A	2σ	($^{232}Th/^{238}U$)A	2σ	($^{230}Th/^{232}Th$)A	Corrected age (ka)	2σ
Monte Tondo - Re Tiberio	**Abisso Mezzano**	**RT-AI r**	0.037	1483	0.6542	0.0049	0.946	0.004	0.000454	0.000001	1440	**130.58**	2.39
		RT-A1 bis	0.015	848	0.6541	0.0043	0.945	0.002	0.000657	0.000006	995	**131.10**	1.87
		RT-A1	0.106	1023	0.6558	0.0012	0.945	0.002	0.000848	0.000007	774	**131.74**	0.75
		RT 2015 1	0.020	1554	0.6490	0.0035	0.944	0.002	0.000402	0.000003	1616	**129.04**	1.53
		RT 2015 5	0.019	1656	0.6572	0.0039	0.956	0.002	0.000607	0.000003	1082	**128.67**	1.65
		RT-B1	0.009	934	0.6541	0.0044	0.956	0.003	0.000239	0.000005	2733	**127.57**	1.83
		RT 2015 7	0.019	1623	0.6510	0.0028	0.957	0.003	0.000730	0.000004	892	**125.77**	1.28
		RT-B I	0.010	1797	0.6479	0.0052	0.952	0.008	0.000125	0.000001	5174	**126.24**	3.20
		RT-B2	0.008	1068	0.6541	0.0039	0.962	0.003	0.000517	0.000006	1266	**125.87**	1.64
		RT-C1	0.010	1004	0.6562	0.0046	0.965	0.003	0.000599	0.000007	1095	**125.58**	1.85
		RT-CI	0.012	1748	0.6498	0.0055	0.958	0.002	0.000075	0.000002	8677	**125.35**	2.11
		RT-C m1	0.013	3127	0.6472	0.0025	0.957	0.002	0.000098	0.000001	6606	**124.95**	1.08
		RT-C m2	0.017	1619	0.6422	0.0020	0.949	0.002	0.000295	0.000003	2176	**125.14**	0.91
		RT-CII	0.012	1669	0.6389	0.0053	0.951	0.002	0.000250	0.000003	2552	**123.45**	2.02
		RT 2015 10	0.020	1696	0.6508	0.0032	0.963	0.002	0.000146	0.000001	4448	**124.36**	1.32
		RT-C2	0.015	972	0.6450	0.0028	0.953	0.002	0.000215	0.000003	3004	**125.17**	1.23
		RT-DI	0.033	1764	0.6461	0.0049	0.955	0.001	0.000682	0.000003	948	**124.74**	1.85
		RT-D III	0.050	1899	0.6484	0.0048	0.961	0.003	0.000684	0.000003	948	**123.94**	1.94
	3 Anelli	**3A**	0.014	2970	0.5932	0.0025	0.946	0.002	0.002052	0.000027	289	**108.86**	0.98
		3A-2016-2	0.045	534	0.6016	0.0024	0.960	0.002	0.005345	0.000025	113	**107.69**	1.28
		3A–t	0.020	1157	0.6223	0.0037	0.968	0.003	0.038551	0.000421	16	**106.29**	7.23
	Abisso 50	**A501**	0.008	1681	0.5176	0.0025	0.970	0.002	0.033461	0.000349	15	**77.89**	6.06
		A502	0.011	1867	0.4843	0.0024	0.965	0.002	0.002576	0.000037	188	**76.10**	0.75
		A503	0.010	955	0.4829	0.0024	0.975	0.002	0.001806	0.000019	267	**74.69**	0.68
	Pozzo Pollini	**D3**	0.100	513	0.5378	0.0021	0.973	0.002	0.002398	0.000013	224	**87.80**	0.70
		PP	0.015	295	0.5207	0.0045	0.976	0.003	0.002766	0.000019	188	**83.14**	1.24
		PP1	0.009	795	0.5201	0.0029	0.970	0.002	0.018004	0.000116	29	**81.18**	3.23
		D2	0.100	652	0.4886	0.0009	0.950	0.001	0.008241	0.000022	59	**77.90**	1.40
		D4	0.100	670	0.4912	0.0013	0.957	0.001	0.008062	0.000030	61	**77.70**	1.40
		PP2	0.017	1165	0.4859	0.0028	0.968	0.002	0.007278	0.000078	67	**75.21**	1.44
	Grotta Oliver	**GO1**	0.012	1217	0.0921	0.0009	0.949	0.002	0.023011	0.000284	4	**7.10**	4.10
		GO2	0.010	924	0.0962	0.0007	0.943	0.002	0.026957	0.000186	4	**6.96**	4.92
		GO-2016-2	0.044	1205	0.0670	0.0004	0.939	0.002	0.017181	0.000321	4	**5.03**	3.09
	Galleria Principale	**RTy 1**	0.047	1511	0.0052	0.0002	0.960	0.001	0.000451	0.000008	12	**0.52**	0.08
		RTy 2	0.045	1432	0.0035	0.0002	0.960	0.001	0.000613	0.000014	6	**0.29**	0.11
		RTy 3	0.051	1548	0.0042	0.0001	0.982	0.002	0.002122	0.000050	2	**0.11**	0.36

(*Continues*)

Table 1. (Continued)

Cave system	Cave	Sample ID	Mass (g)	^{238}U (ng/g)	($^{230}Th/^{238}U$)A	2σ	($^{234}U/^{238}U$)A	2σ	($^{232}Th/^{238}U$)A	2σ	($^{230}Th/^{232}Th$)A	Corrected age (ka)	2σ
Spipola - Acquafredda	**Spipola**	**Spd-2016-1**	0.047	924	1.0480	0.0042	1.126	0.002	0.000147	0.000002	7124	**253.90**	4.41
		SpD-E	0.120	586	0.9303	0.0097	1.026	0.009	0.000416	0.000004	2238	**252.10**	14.77
		SpD-D	0.118	442	0.9061	0.0104	1.009	0.010	0.002357	0.000026	384	**246.63**	16.16
		SpD-C	0.049	1003	1.0197	0.0064	1.112	0.004	0.000020	0.000001	50924	**243.58**	6.52
		SpD-B	0.051	3052	1.0215	0.0051	1.111	0.004	0.000004	0.000000	277192	**245.55**	5.64
		SpD-A	0.050	1971	1.1318	0.0055	1.207	0.004	0.000465	0.000009	2432	**246.34**	5.31
		SpD b	0.063	429	0.9245	0.0035	1.028	0.002	0.000264	0.000002	3506	**243.53**	3.97
		Spd-2016-2	0.048	484	0.8964	0.0035	1.007	0.002	0.002002	0.000039	448	**239.34**	4.30
		Sp1-b	0.038	736	0.0170	0.0004	1.029	0.003	0.007400	0.000186	2	**0.63**	1.19
		Sp1-t	0.034	731	0.0071	0.0002	1.024	0.003	0.003287	0.000071	2	**0.23**	0.53
		SpS-b	0.044	1012	0.0143	0.0003	1.045	0.002	0.001267	0.000025	11	**1.30**	0.20
		SpS-t	0.045	1062	0.0027	0.0002	1.031	0.002	0.000901	0.000015	3	**0.14**	0.14
Castelnuovo	**Peroni**	**P2-b**	0.039	989	0.0818	0.0007	0.984	0.003	0.009378	0.000174	9	**7.89**	1.58
		P2-t	0.036	1120	0.0389	0.0004	1.048	0.003	0.000289	0.000005	135	**4.08**	0.06
		P3-B	0.035	1435	0.0479	0.0009	1.014	0.002	0.000412	0.000011	116	**5.22**	0.12
		P3-T	0.044	1368	0.0246	0.0005	1.057	0.002	0.000071	0.000001	347	**2.56**	0.05
	Mornig	**MOR2-b**	0.020	1314	0.0424	0.0006	0.880	0.002	0.012795	0.000034	3	**2.99**	2.44
		MOR2-t	0.021	2313	0.0218	0.0003	0.857	0.003	0.001254	0.000005	17	**2.57**	0.24
Stella - Rio Basino	**Rio Basino**	**RBT-b**	0.049	1076	0.0588	0.0005	0.893	0.003	0.013927	0.000202	4	**4.84**	2.64
		RBT-t	0.052	1102	0.0432	0.0005	0.887	0.003	0.008033	0.000094	5	**3.95**	1.51
		RB3-b	0.050	511	0.0252	0.0005	0.937	0.003	0.004679	0.000060	5	**2.15**	0.83
		RB3-t	0.050	492	0.0089	0.0004	0.950	0.003	0.003228	0.000060	3	**0.47**	0.56
		RB1-b	0.034	569	0.0612	0.0013	0.935	0.002	0.011802	0.000275	5	**5.29**	2.11
		RB1-t	0.042	494	0.0282	0.0008	0.953	0.002	0.010104	0.000227	3	**1.53**	1.77
Monte Mauro	**Monte Mauro**	**MM2-b**	0.039	731	0.9225	0.0042	0.981	0.003	0.019454	0.000541	47	**316.17**	12.65
		MM2-t	0.034	1367	0.8783	0.0031	0.990	0.003	0.001359	0.000028	646	**239.98**	4.46
		MM4 b	0.021	556	0.9782	0.0062	0.994	0.003	0.001776	0.000010	551	**468.00**	+130/−42
		MM4 t	0.023	393	0.9375	0.0060	0.995	0.003	0.002130	0.000009	440	**313.44**	14.27
	Banditi	**BA 1.1**	0.050	1071	0.9988	0.0051	0.998	0.004	0.111054	0.000331	9	> **580**	-
		BA 2.1	0.050	804	0.9569	0.0045	0.991	0.004	0.001508	0.000023	635	**378.00**	+29/−20
		BA_BIG_1	0.075	1837	0.6804	0.0026	0.976	0.004	0.000010	0.000000	69553	**131.29**	1.46
		BA_BIG_2	0.069	886	0.6776	0.0030	0.987	0.003	0.000011	0.000001	62589	**127.07**	1.40
		BA_BIG_3	0.066	706	0.6563	0.0029	0.990	0.003	0.000039	0.000001	16700	**119.01**	1.26
		BA_BIG_4	0.070	979	0.6363	0.0026	0.990	0.003	0.000462	0.000007	1377	**112.36**	1.09

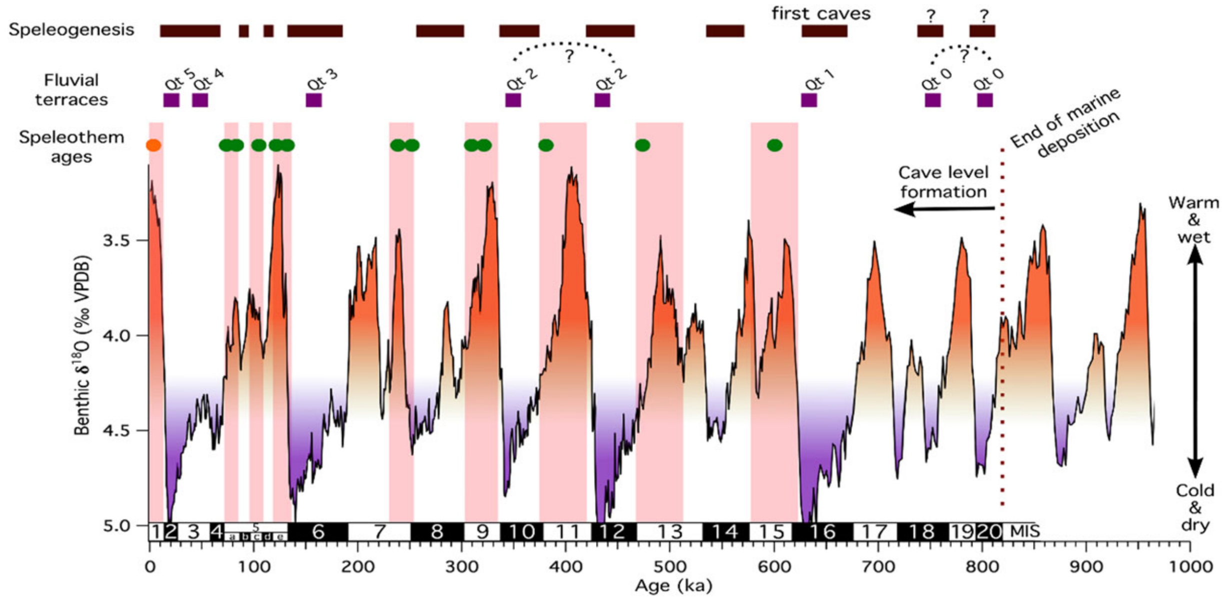

Figure 4. Speleogenetic processes over the last ~800 ka. Circles indicate the basal ages of the studied speleothems (except for the sample Ba2 at ~380 ka, which reported only the top age; Holocenic ages are aggregated in a single circle). The ages mainly fit with periods of warm and wet climate (vertical shading). The formation of the different cave levels (rectangles) is correlated with the first cold–dry climate stage (purple shading) occurred before the warm–wet period indicated by the age of the speleothems (see Figure 6 and text), simultaneous with the deposition of most of the fluvial terrace sediments along the main river of the area (squares) (Cyr and Granger, 2008; Picotti and Pazzaglia, 2008; Wegmann and Pazzaglia, 2009). The climatic curve refers to the δ18O benthic stack of Lisiecki and Raymo (2005). First caves were carved at least ~630 kyr ago. [Colour figure can be viewed at wileyonlinelibrary.com]

average age, MIS 12 to 15 considering the error) and the top at 313.44 ± 14.27 ka (MIS 9), MM2 bottom is at 316.17 ± 12.65 ka (MIS 9) and the top at 239.98 ± 4.46 ka (MIS 7e). Although intermediate ages between the bottom and the top of these last two speleothems were not done, petrographic evidence shows that the deposition of the carbonate was not continuous but characterised by growth interruptions. Ba1 and Ba2, belonging to the same karst system, report only one age each, respectively, at 689 ± 369.10 ka (bottom age) and 378.26 ± $^{+29}/_{-20}$ ka (top age). Despite the large uncertainty, we are 95% confident that Ba1 is older than 580 ka, and might coincide with MIS 15. Ba2 instead might fit with the latest part of MIS 11.

Discussion

Messinian gypsum caves in South Spain formed in a semi-confined aquifer since the lower Pleistocene (Calaforra and Pulido-Bosch, 2003). Marly strata intercalated with gypsum beds drove the speleogenesis creating the first proto-conduits under phreatic conditions, which later developed into a multi-level cave system following river entrenchment and vadose erosion. Field evidence testify to this process, such as 'V' shaped passages, meandering braided pendants, ceiling channels and gypsum layer breakdown in the cave roofs as relict of the ancient speleogenetic evolution (Calaforra and Pulido-Bosch, 2003). The situation is quite different in our area of study. All cave levels are ~horizontal, while the gypsum sequence is tilted (from 20° to 45°, De Waele and Pasini, 2013). This means that marly strata did not control speleogenesis. We recently demonstrated that the formation of caves composing the Monte Tondo karst system was related to climate-driven base level oscillations over the last ~130 000, and occurred in an unconfined aquifer (Columbu *et al.,* 2015). The formation of epigenic caves in macrocrystalline gypsum is only possible once the soluble rocks emerge and are in contact with undersaturated fresh water. The *Vena del Gesso* gypsum formation was originally covered by marine silts and clays of the *Argille Azzurre* (sky-blue clays) formation (Amorosi *et al.*, 1998), deposited from ~5.3 Ma to ~1.8 Ma, followed by the *Sabbie Gialle* (yellow sands) formation (Antoniazzi *et al.*, 1993; Cyr and Granger, 2008) (Figure 5). The latter is mostly comprised of littoral marine sandstone (Marabini *et al.*, 1995) deposited during Early Pleistocene phases of sea-level high stands. The top age of the *Sabbie Gialle* is attested at 780–820 ka, provided by electron spin resonance and palaeomagnetic calculations (Antoniazzi *et al.*, 1993; Falgueres, 2003; Muttoni *et al.*, 2011). This age (~800 ka) marks the beginning of the so-called 'continental Quaternary' (Benini *et al.*, 1999; Amorosi *et al.*, 2015), which in the local sequence stratigraphy comprises all sediments deposited after the definitive regression of the Adriatic Sea. From a speleogenetic perspective, it defines the potential maximum age for the beginning of the development of the oldest epigenic caves. The emergence of the Apennine piedmont resulted from the rapid uplifting of the area, calculated at 0.2–0.3 mm per year around the middle Pleistocene (Cyr and Granger, 2008; Picotti and Pazzaglia, 2008). The retreat of the shoreline was possibly fuelled by the Middle Pleistocene Transition (Pisias and Moore, 1981; Muttoni *et al.*, 2003; Maslin and Ridgwell, 2005), after which the severity of glaciations increased.

It is unlikely that speleogenesis started as soon as the sea retreated. All caves show epigenic morphology, characterised by typical gypsum through-flow conduits (Klimchouk, 2000). A sub-horizontal cave tunnel is excavated parallel to the piezometric level at the same altitude as the base level. This implies that: (i) the majority of the sediments originally covering the gypsum karst terrain (i.e. Argille Azzurre clays and Imola sands) were removed before commencement of the epigenic speleogenesis; and (ii) the superficial drainage system already developed a certain status of maturity, sustaining the valley incision and creating the altitudinal gradient necessary for the flow of the groundwater (Figure 5). The oldest river terrace (Qt0) preserved along the Bidente and Reno valleys, located respectively to the north and to the south of the study area,

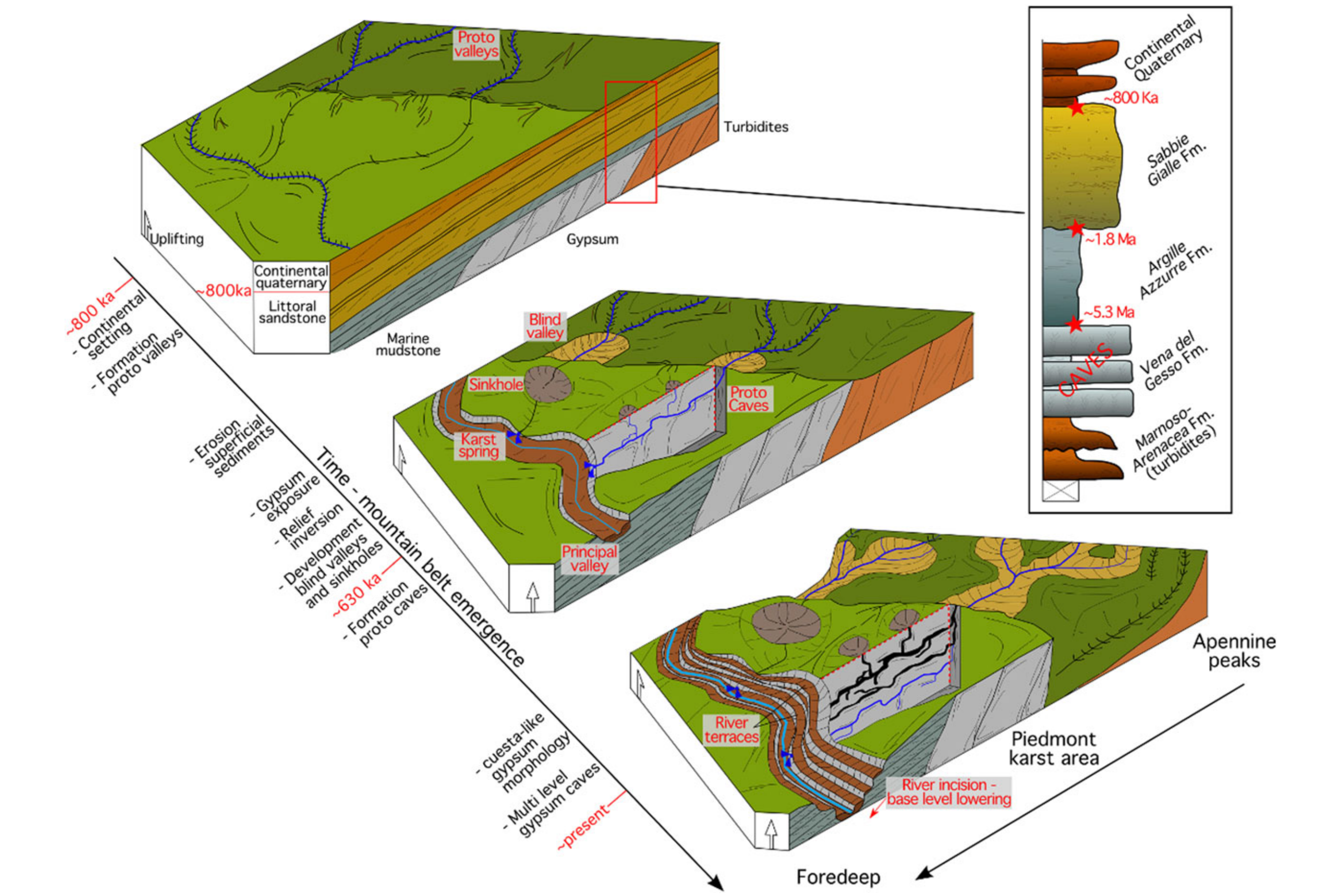

Figure 5. Geological, geomorphological and speleogenetic evolution of the study area and original stratigraphic succession of the Apennine piedmont (small inbox). Speleogenetic processes could only start after exhumation of the area (~800 ka), triggered by the rapid regional uplifting. The gypsum sequence was exposed after the erosion of most of the superficial sediments. The exposure of gypsum facilitated sinkholes and the blind valley formation, which conveyed the water underground. The first caves were thus formed at ~630 ka (see text). The cyclical lowering/stasis of the local base level was decisive for the creation of multiple sub-horizontal cave levels (underground section indicated by the dotted red line) and deposition of the river terraces (see Figure 6). Currently gypsum outcrops with a typical cuesta-like morphology, due to the phenomenon of the relief inversion. Note that, for simplicity, the tectonic features reported in this scheme are only indicative. [Colour figure can be viewed at wileyonlinelibrary.com]

has no numerical ages (Figure 4). Through stratigraphical correlation with the equivalent Po Plain foredeep sediments, it is tentatively assigned to one of the MIS 22, MIS 20, or MIS 18 glaciation peaks (Cyr and Granger, 2008; Picotti and Pazzaglia, 2008; Wegmann and Pazzaglia, 2009), respectively at ~870, ~800 and ~740 ka. Thus, proto valleys already developed at least by ~740 ka, which is 60–80 kyrs after the definitive emergence of the area. However, the hydrological network was possibly fully efficient between 400 and 500 ka, when the first alluvial fans were deposited in the Padana foredeep (Gunderson *et al.*, 2014; Amorosi *et al.*, 2015).

When comparing the minimum ages of the samples with global climatic variations over the last ~800 ka (Lisiecki and Raymo, 2005), it is worth noting that the presence of carbonate speleothems coincides with stages of climate optima (Figure 4), in line with our previous work based on the speleothems from Monte Tondo (Columbu *et al.*, 2015). Speleothems were mainly formed during the peak interglacial periods (Holocene, MIS5e, MIS7e, MIS9, MIS11), with two of them potentially linkable to MIS13 (MM4 flowstone) and MIS 15 (Ba1). Although interglacials do vary in terms of duration, average temperatures and rainfall dynamics (Tzedakis *et al.*, 2009), these periods are recognised as the emblems of considerably warm and wet climate (Sirocko *et al.*, 2006). The influence of climate on the deposition of the speleothems is also evident in an intraglacial/interglacial timescale. GO, PP and A50 flowstones formed during the Greenland interstadials (GIS) 24, 21, and 20, respectively (Figure 4). GIS are rapid returns to an interglacial-like climate (although generally less warm) during an otherwise glacial period (Dansgaard *et al.*, 1993). Enhanced rainfall and humidity is the most suitable condition for the development of pervasive vegetation in the piedmont hillslopes. From a geochemical point of view, this means that the overabundance of biogenic CO_2 released by the pedogenic layers at the surface has a key impact in the production of carbonate speleothems once the waters percolate into the gypsum caves (Borsato *et al.*, 2015).

From a geomorphological perspective, a thicker vegetation cover protects the hillslopes from surface erosion during these warmer and wetter periods. The availability of sediments on the slopes is reduced when compared with relatively colder climates. In southern Italy, pollen data indicate that glacial climates favoured the expansion of steppe-like and bush vegetation (Allen and Huntley, 2009). In this circumstance, the bedrock is largely exposed to weathering processes; the resulting regolith is gravitationally conveyed toward the bottom of the slopes, usually constituted by the active base level valley (Simoni *et al.*, 2013). Considering the latitudinal difference between the southern side of the peninsula and the northern Apennines, it is probable that in the studied area this vegetation persisted beyond the peak of the glaciations, prolonging conditions conducive to maximum regolith production.

The fluvial terraces preserved in the main rivers draining the northern Apennines (Bidente and Reno rivers) were all formed during these periods of abundant regolith production (Wegmann and Pazzaglia, 2009) (Figure 4). Besides the aforementioned Qt0 generation, terrace Qt1 correlates with MIS16, Qt2 with MIS12 or MIS10, Qt3 with MIS6, Qt4 with MIS4 and Qt5 with MIS2 (younger fluvial terraces are also known from the Holocene, but are not reported in Figure 4). The presence of a terrace deposit is evidence that the river maintained a ~ stable palaeo-altitudinal position necessary for the aggradation of the slope sediments in the river trunk. These periods of stability were longer than 1000 years (Wegmann and Pazzaglia, 2009); the alluviated valleys were incised by a lowering of the base level under a different climate regime. The epigenic karst systems are strictly connected to the local base-level variation. When the base level lowers, karstification proceeds vertically, in the same way rivers entrench the valley bottoms. The Apennine gypsum karst shows evidence of this process through deep and narrow shafts; in the Monte Tondo cave network, the *Pozzo Pellegrini* shaft is more than 30 m deep (De Waele *et al.*, 2013). In contrast, when the river establishes a new altitudinal position, underground waters run according to the new piezometric level. The accumulation of slope sediments forms alluvial valleys that, at the millennial scale, act as new stable base levels for the karst systems. The main sub-horizontal cave tunnels are thus excavated during these stable time intervals.

Five superimposed cave levels are particularly well preserved in the Monte Tondo-Re Tiberio karst system. Further evidence for the connection between the fluvial dynamics and speleogenetic processes is the presence of paragenetic canyons in several of the cave ceilings (Pasini, 1966, 1967, 1973). When the supply of slope material exceeds the maximum bedload sustainable by the river flow, aggradation occurs in the valley bottom pushing the local base level slowly upward. In response, underground conduits also accumulate sediments and the running waters erode the cave ceilings through so-called antigravitative erosion process (Pasini, 2009). Taking into account the cyclical stability of the base level witnessed by the river terraces and the stacked-like nature of the gypsum karst systems carved in the north Apennine piedmont, we attribute the excavation of the sub-horizontal cave tunnels to periods of relative colder climate (Figures 4 and 6). River terraces are present at the same altitude as the main cave levels of the studied area (Columbu *et al.*, 2015). Although they have not always been dated, their formation should correspond to the same genetic dynamics controlling the hydrogeology of the area (Wegmann and Pazzaglia, 2009), being deposited during cold stages. However, the ages of the speleothems provide an indication of the minimal age of the cave tunnels (and thus the related terraces). When terraces and caves are in the formation stage, the result is underground passages completely filled by water, and vadose speleothem deposition is not possible. Once these new caves are drained, following renewed entrenchment of the river, speleothem formation can start (Columbu *et al.*, 2015). Because cold periods favouring the excavation of the cave voids are followed by warm periods favouring speleothem deposition, it is feasible to assign the speleogenesis of a certain cave level to the first cold period preceding the oldest speleothem age sampled in that cave (Figure 6).

It could be argued that speleothems might have formed even thousands of years after the drainage of the cave, confounding our understanding of the age of speleogenesis. This cannot, of course, be excluded in this study. However, there is good agreement between the antiquity of the speleothems and the altitude of the caves in which they were found (Figure 7). In the Monte Tondo-Re Tiberio system, RT flowstone – recovered at ~340 m a.s.l. – was deposited ~130 kyr ago (Columbu *et al.*, 2015). The speleothems sampled close to the actual base level

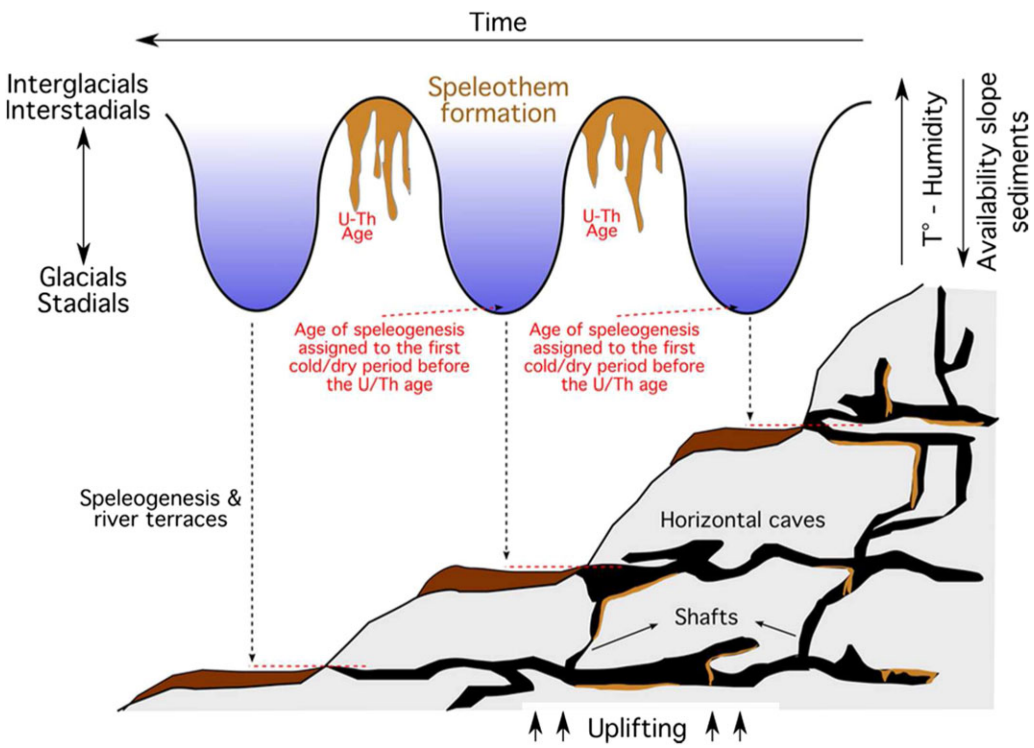

Figure 6. Schematic model of the formation of sub-horizontal cave levels and fluvial terraces in relation to cyclic climate changes. River terraces, formed during cold climates, record periods of stability in the palaeo base level longer than 1000 years (Wegmann and Pazzaglia, 2009). Contemporaneously, sub-horizontal cave tunnels are carved at the same altitude. The oldest generation of speleothems at a certain cave are deposited when the new-born cave reaches a vadose status, during periods of relatively warm climates. The first cold period before the warm stage indicated by the speleothems is considered as the minimum age for the formation of the caves. [Colour figure can be viewed at wileyonlinelibrary.com]

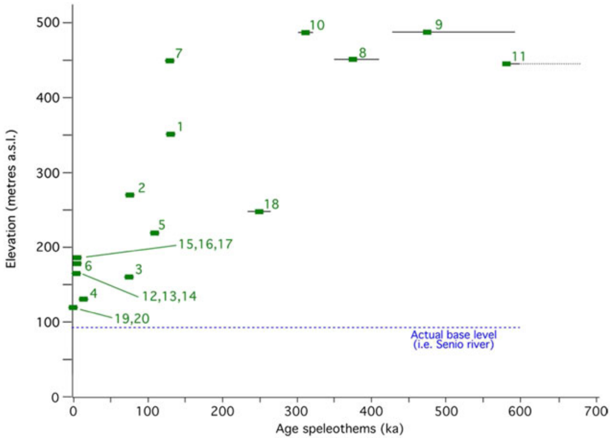

Figure 7. Age vs altitude for the speleothems used in this study. Horizontal bars are the 2σ uncertainties associated with the basal ages. Despite a few outliers, the antiquity of the speleothems generally correlates with the altitude of the cave level or cave entrance where they were found. Numbers refer to Figure 3. [Colour figure can be viewed at wileyonlinelibrary.com]

in the cave (~95 m a.s.l.) were Holocene in age. Those speleothems sampled in between these two cave levels report intermediate ages. In general, all the oldest speleothems come from the highest-altitude cave levels. The speleothems older than 300 ka, from the Monte Mauro system, have all been recovered at altitudes higher than 400 m a.s.l., the most elevated portions of the Apennine foothills (Figure 7). Thus the chronology of the speleothem production follows an altitudinal gradient, which in turn mirrors the progressive base level-driven downward migration of the speleogenetic processes.

The oldest speleothems in our collection provides a basal age of >580 ka (Ba1) and 468.00 $^{+130}/_{-42}$ ka (MM4 flowstone). This suggests that caves already existed in the area at least since MIS15 (i.e. ~600 kyrs ago, justified by Ba1 age and the oldest possible MM4 age). Assigning the timing of speleogenesis to the coldest period just before MIS15 (MIS16), the excavation of the first caves probably occurred at least 630 kyr ago, ~200 kyr after the complete emergence of the area. This timespan (~200 kyr) appears sufficiently long for several reasons. First, there is adequate time for the erosion of the majority of the marine sediments covering the area and the gypsum beds, fuelled by the rapid uplifting of the area. Currently, in many watersheds, these sediments are visible as uplifted fluvial terraces (Picotti and Pazzaglia, 2008; Wegmann and Pazzaglia, 2009). Second, it is a reasonable timeframe for the formation of a drainage network, which will later develop into deep river valleys. The age of the caves at ~630 ka is very close to the time of the formation of the first alluvial fan in the Padana foredeep (Gunderson *et al.*, 2014; Amorosi *et al.*, 2015), symptomatic of the general maturity of the fluvial system. Finally, there is sufficient time for triggering the geomorphological phenomenon known as ‘relief inversion’ (Pain and Oilier, 1995) (Figure 5). Nowadays, gypsum beds stand out as prominent cuesta-like ridges because of the differential erosion of the adjacent formations (De Waele *et al.*, 2012b) (Figure 2(B)). Whereas in the non-soluble terrains surface erosion leads to a progressive lowering of the ground level, enhanced by the rapid uplifting of the area, in gypsum the bulk of the erosion is transferred underground. When gypsum was first exposed, the rivers descending from the upper part of the foothills penetrated the karst rocks, initiating blind valleys at the contact between soluble and non-soluble terrains (Figure 5). The Rio Stella blind valley is today an excellent example of this style of surface versus subterraneous drainage (De Waele, 2010). Sinkholes also facilitated the penetration of water into the karst systems. The large Spipola doline close to Bologna, with a diameter of more than 500 m, is one of the most striking examples (Forti and Sauro, 1996) (Figure 2(A)). Around 600 years ago, the first proto-caves transferred surface water into the downstream main river throughout karst springs, at least in the Monte Mauro and Banditi caves where MM4 and Ba1 flowstone were found. Large portions of these first caves have now been disaggregated. At the same time the flowstone collected in the Spipola doline (close to Bologna), dated at ~250 ka, testifies to the formation of the caves in this area from at least 260 000 years ago; these old caves, probably forming the upper levels of the current levels constituting the Spipola-Acquafredda system, have also been eroded.

Conclusions

This study reports the U–Th radiometric dating of twenty carbonate speleothems sampled in the Messinian gypsum karst areas of the northern Apennines. In agreement with previous work based on speleothems recovered from the Monte Tondo-Re Tiberio karst system, the age of the samples fits with periods of warm and wet climate. Specifically, the speleothems correlate with the current (Holocene) and previous interglacials (MIS 5e, 7e, 9, 11, 13 and probably 15) and the Greenland interstadials 24, 21 and 20. The basal age of the speleothems provides an indication of the minimum age of the cave passages in which they are found. The age of the speleothems found at the surface is evidence for the presence of past cave levels that have been partially or completely destroyed by surface denudation. The main sub-horizontal cave tunnels constituting the explored karst system formed when the palaeo-base level stabilized at a new altitudinal position during cold–dry climate stages. In these periods, vegetation-free hillslopes saw high amounts of regolith transported downslope to the trunk river valley, after which subsequent incision formed river terraces at the same altitude as the cave levels. The available ages of the river terrace formations in the area corroborate the correlation between speleogenesis and periods of relatively cold and dry climate. Considering the age of the speleothems, the formation of the associated cave passages were assigned to the cold–dry climate stage immediately before the warm–wet phase attributed to speleothem growth.

This study has important implications for understanding the timing of underground and surface drainage systems development in rapidly uplifting areas. First, it reviewed the duration of speleogenesis in Northern Italian gypsum terrains, which has been underestimated until now. In the Monte Mauro area, caves were already forming at least ~630 000 years ago, 200 000 years after the emergence of the Apennine piedmont. It follows that this time period was necessary for the erosion of most of the sediments covering the gypsum sequence, the incision of the proto valleys and the creation of the karst sinkholes, the latter introducing the majority of surface waters into the subterranean voids. Furthermore, the carving of epigenic caves was enhanced once the phenomenon of relief inversion exposed the gypsum sequence as a karstificable ridge among non-soluble terrains. In the Spipola area close to Bologna, caves were present at least 260 000 years ago. These old cave conduits have mostly been destroyed by surface denudation of the gypsum bedrock, while the carbonate speleothems that decorated their walls/floors have been better preserved and can still be found scattered across the surface.

Acknowledgements—We thank the GAM Mezzano, GSB/USB Bologna and GSFa that partially financed this project. We are grateful to Garibaldi (Baldo) Sansavini, Massimo Ercolani, Piero Lucci, Luca Grillandi, Roberto Evilio, Katia Poletti, Alessandro Pirazzini, Alan Nardi, Luca Tarozzi, Michele Castrovilli, Roberto Cortelli, Francesco Grazioli, Fabio Giannuzzi and Ilenia Maria D'Angeli for their tireless help during the fieldwork. Comments by David Richards and anonymous reviewers, as well as by Professor Lane and an associate editor have helped in improving our manuscript.

References

Allen JRM, Huntley B. 2009. Last Interglacial palaeovegetation, palaeoenvironments and chronology: a new record from Lago Grande di Monticchio, southern Italy. *Quaternary Science Reviews* **28**(15): 1521–1538.

Amorosi A, Caporale L, Cibin U, Colalongo M, Pasini G, Ricci Lucchi F, Severi P, Vaiani S. 1998. The Pleistocene littoral deposits (Imola Sands) of the northern Apennines foothills. *Giornale di Geologia* **60**: 83–118.

Amorosi A, Maselli V, Trincardi F. 2015. Onshore to offshore anatomy of a late Quaternary source-to-sink system (Po Plain–Adriatic Sea, Italy). *Earth-Science Reviews* **153**: 212–237.

Antoniazzi A, Ferrari M, Peretto C. 1993. Il giacimento di Ca'Belvedere di Monte Poggiolo del Pleistocene inferiore con industria litica (Forlì). *Bullettino di Paletnologia Italiana* **84**: 1–56.

Audra P, Bini A, Gabrovšek F, Häuselmann P, Hobléa F, Jeannin P-Y, Kunaver J, Monbaron M, Šušteršić F, Tognini P. 2006. Cave genesis in the Alps between the Miocene and today: a review. *Zeitschrift für Geomorphologie* **50**(2): 153–176.

Audra P, Lauritzen SE, Rochette P. 2011. Speleogenesis in the hyperkarst of the Nakanai Mountains (New Britain, Papua New-Guinea). Evolution model of a juvenile system (Muruk Cave) inferred from U/Th and paleomagnetic dating. *Speleogenesis and Evolution of Karst Aquifers* **10**: 25–30.

Bajo P, Drysdale R, Woodhead J, Hellstrom J, Zanchetta G. 2012. High-resolution U–Pb dating of an Early Pleistocene stalagmite from Corchia Cave (central Italy). *Quaternary Geochronology* **14**: 5–17.

Balestrieri M, Bernet M, Brandon MT, Picotti V, Reiners P, Zattin M. 2003. Pliocene and Pleistocene exhumation and uplift of two key areas of the Northern Apennines. *Quaternary International* **101**: 67–73.

Benini A, Martelli L, Amorosi A, Martini A, Severi P, Cazzoli MA, Vaiani SC. 1999. Note illustrative della carta geologica d'Italia alla scala 1:50.000. Servizio Geologico d'Italia, Roma.

Borsato A, Frisia S, Miorandi E. 2015. Carbon dioxide concentration in temperate climate caves and parent soils over an altitudinal gradient and its influence on speleothem growth and fabrics. *Earth Surface Processes and Landforms* **40**(9): 1158–1170.

Calaforra JM, Pulido-Bosch A. 2003. Evolution of the gypsum karst of Sorbas (SE Spain). *Geomorphology* **50**: 173–180.

Calvet M, Gunnell Y, Braucher R, Hez G, Bourlès D, Guillou V, Delmas M, Team ASTER. 2015. Cave levels as proxies for measuring post-orogenic uplift: evidence from cosmogenic dating of alluvium-filled caves in the French Pyrenees. *Geomorphology* **246**: 617–633.

Cheng H, Lawrence Edwards R, Shen C-C, Polyak VJ, Asmerom Y, Woodhead J, Hellstrom J, Wang Y, Kong X, Spötl C, Wang X, Calvin AE. 2013. Improvements in ^{230}Th dating, ^{230}Th and ^{234}U half-life values, and U–Th isotopic measurements by multi-collector inductively coupled plasma mass spectrometry. *Earth and Planetary Science Letters* **371–372**: 82–91.

Chiarini V, Evilio R, De Waele J. 2015. Note di speleogenesi nei gessi di Brisighella e Rontana. *Memorie dell'Istituto Italiano di Speleologia* **II**(28): 113–118.

Columbu A, De Waele J, Forti P, Montagna P, Picotti V, Pons-Branchu E, Hellstrom J, Bajo P, Drysdale RN. 2015. Gypsum caves as indicators of climate-driven river incision and aggradation in a rapidly uplifting region. *Geology* **43**(6): 539–542.

Cyr AJ, Granger DE. 2008. Dynamic equilibrium among erosion, river incision, and coastal uplift in the northern and central Apennines, Italy. *Geology* **36**(2): 103–106.

Dansgaard W, Johnsen SJ, Clausen HB, Dahl-Jensen D, Gundestrup NS, Hammer CU, Hvldberg CS, Steffensen JP, Sveinbjornsdottir AE, Jouzel J, Bond G. 1993. Evidence for general instability of past climate from a 250-kyr ice–core record. *Nature* **364**: 218–220.

De Waele J. 2010. Speleogenesi del complesso carsico di Rio Stella–Rio Basino. In *Il progetto Stella–Basino*, Lucci P, Forti P (eds). *Memorie dell'Istituto Italiano di Speleologia* **II**(23): 95–108.

De Waele J, Pasini G. 2013. Intra-messinian gypsum palaeokarst in the northern Apennines and its palaeogeographic implications. *Terra Nova* **25**(3): 199–205.

De Waele J, Piccini L. 2008. Speleogenesi e morfologia dei sistemi carsici in rocce carbonatiche. In *Atti del 45 Corso CNSS–SSI di III livello di geomorfologia carsica*, Parise M, Inguscio S, Marangella A (eds): Federazione Speleologica Pugliese: Grottaglie; 23–74.

De Waele J, Forti P, Rossi A. 2011. Il carsismo nelle evaporiti dell'Emilia Romagna. In *Speleologia e geositi carsici in Emilia Romagna*, Lucci P, Rossi A (eds). Pitagora: Bologna; 25–59.

De Waele J, Ferrarese F, Granger D, Sauro F. 2012a. Landscape evolution in the Tacchi area (central-east Sardinia, Italy) based on karst and fluvial morphology and age of cave sediments. *Geografia Fisica e Dinamica Quaternaria* **35**: 119–127.

De Waele J, Anfossi G, Campo B, Cavalieri F, Chiarini V, Emanuelli V, Grechi U, Nanni P, Savorelli F. 2012b. Geomorphology of the Castel de'Britti area (Northern Apennines, Italy): an example of teaching geomorphological mapping in a traditional and practical way. *Journal of Maps* **8**(3): 231–235.

De Waele J, Fabbri F, Forti P, Lucci P, Marabini S. 2013. Evoluzione speleogenetica del sistema carsico del re Tiberio (Vena del gesso Romagnola). *Memorie dell'Istituto Italiano di Speleologia* **II**(26): 81–101.

Demaria D. 2002. Emilia Romagna. In *Le Aree Carsiche Gessose D'Italia*, Madonia G, Forti P (eds). *Memorie dell'Istituto Italiano di Speleologia* **II**(14): 159–184.

Drysdale RN, Bence TB, Hellstrom JC, Couchoud I, Greig A, Bajo P, Zanchetta G, Isola I, Spötl C, Baneschi I, Regattieri E, Woodhead JD. 2012. Precise microsampling of poorly laminated speleothems for U-series dating. *Quaternary Geochronology* **14**: 38–47.

Emiliani C. 1955. Pleistocene temperatures. *Journal of Geology* **63**: 538–578.

Fairchild IJ, Baker A. 2012. Appendix 1: Archiving speleothems and speleothem data. In *Speleothem Science: From Process to Past Environments*, Fairchild IJ, Baker A (eds). Wiley–Blackwell: Chichester; 368–370.

Falgueres C. 2003. ESR dating and the human evolution: contribution to the chronology of the earliest humans in Europe. *Quaternary Science Reviews* **22**: 1345–1351.

Farrant AR, Smart PL, Whitaker FF, Tarling DH. 1995. Long-term quaternary uplift rates inferred from limestone caves in Sarawak, Malaysia. *Geology* **23**(4): 357–360.

Ford D, Williams P. (eds). 2007. *Karst Geomorphology and Hydrology*. John Wiley & Sons: Chichester.

Forti P. 2003. I sistemi carsici. In *Risposta dei processi geomorfologici alle variazioni ambientali*, Biancotti A, Motta M (eds). Briganti: Genova; 246–251.

Forti P, Chiesi M. 2001. Idrogeologia, idrodinamica e meteorologia ipogea dei Gessi di Albinea, con particolare riguardo al Sistema carsico afferente alla Tana della Mussina di Borzano (ER–RE 2) (Albinea–Reggio Emilia). *Memorie dell'Istituto Italiano di Speleologia* **II**(11): 115–139.

Forti P, Sauro U. 1996. The gypsum karst of Italy. *International Journal of Speleology* **25**(3–4): 239–250.

Gunderson KL, Pazzaglia FJ, Picotti V, Anastasio DA, Kodama KP, Rittenour T, Frankel KF, Ponza A, Berti C, Negri A. 2014. Unraveling tectonic and climatic controls on synorogenic growth strata (Northern Apennines, Italy). *Geological Society of America Bulletin* **126**(3–4): 532–552.

Häuselmann P, Mihevc A, Pruner P, Horáček I, Čermák S, Hercman H, Sahy D, Fiebig M, Zupan Hajna N, Bosák P. 2015. Snežna jama (Slovenia): interdisciplinary dating of cave sediments and implication for landscape evolution. *Geomorphology* **247**: 10–24.

Hellstrom J. 2003. Rapid and accurate U/Th dating using parallel ion-counting multi-collector ICP–MS. *Journal of Analytical Atomic Spectrometry* **18**: 1346–1351.

Hellstrom J. 2006. U-Th dating of speleothems with high initial ^{230}Th using stratigraphical constraint. *Quaternary Geochronology* **1**(4): 289–295.

Klimchouk AB. 2000. Speleogenesis in noncarbonate lithologies. In *Speleogenesis, Evolution of Karst Aquifers*, Klimchouk AB, Ford DC, Palmer AN, Dreybrodt W (eds). National Speleological Society: Huntsville; 430–442.

Klimchouk AB. 2007. Hypogene speleogenesis: hydrogeological and morphogenetic perspective. National Cave and Karst Research Institute, Carlsbad. Special Paper № 1, Carlsbad.

Klimchouk AB. 2012. Ukraine Giant Gypsum Caves. In *Encyclopedia of Caves*, Gunn J (ed). Fitzroy Dearborn: New York; 827–833.

Krijgsman W, Hilgen F, Raffi I, Sierro F, Wilson D. 1999. Chronology, causes and progression of the Messinian salinity crisis. *Nature* **400**(6745): 652–655.

Lisiecki LE, Raymo ME. 2005. A pliocene–pleistocene stack of 57 globally distributed benthic δ ^{18}O records. *Paleoceanography* **20**(1): 1–17.

Lugli S, Manzi V, Roveri M, Scheiber BC. 2010. The primary lower gypsum in the mediterranean: a new facies interpretation for the first stage of the Messinian salinity crisis. *Palaeogeography Palaeoclimatology Palaeoecology* **297**(1): 83–99.

Marabini S, Taviani M, Vai GB, Vigliotti L. 1995. Yellow sand facies with *Arctica Islandica*: low stand signature in an early pleistocene front–apennine basin. *Giornale di Geologia* **57**(1–2): 259–275.

Maslin MA, Ridgwell AJ. 2005. Mid-pleistocene revolution and the 'eccentricity myth'. *Geological Society, London, Special Publications* **247**(1): 19–34.

Miari M. 2007. L'eneolitico. In *Archeologia dell'Apennino Romagnolo: il Territorio di Riolo Terme*, Guarnieri C (ed). Imola; 30–33.

Muttoni G, Carcano C, Garzanti E, Ghielmi M, Piccin A, Pini R, Rogledi S, Sciunnach D. 2003. Onset of major Pleistocene glaciations in the Alps. *Geology* **31**(11): 989–992.

Muttoni G, Scardia G, Kent DV, Morsiani E, Tremolada F, Cremaschi M, Peretto C. 2011. First dated human occupation of Italy at ~0.85 Ma during the late Early Pleistocene climate transition. *Earth and Planetary Science Letters* **307**(3–4): 241–252.

Negrini C. 2007. Re Tiberio. In *Archeologia dell'Apennino Romagnolo: il Territorio di Riolo Terme*, Guarnieri C (ed). Imola; 51–52.

NGRIP, North Greenland Ice Core Project Members. 2004. High-resolution record of Northern Hemisphere climate extending into the last interglacial period. *Nature* **431**(7005): 147–151.

Pain C, Oilier C. 1995. Inversion of relief – a component of landscape evolution. *Geomorphology* **12**(2): 151–165.

Pasini G. 1966. I canali di volta nelle grotte carsiche del Bolognese. Nuove ipotesi sulla loro formazione: Unpublished Graduation Short Experimental Thesis. Library Dept. Earth and Geoenvironmental Sciences of the Bologna University, 280, 83.

Pasini G. 1967. Osservazioni sui canali di volta delle grotte bolognesi. *Le Grotte d'Italia* **IV**(1): 17–74.

Pasini G. 1969. Fauna a mìammiferi del Pleistocene superiore in un paleoinghiottitoio carsico presso Monte Croara (Bologna). *Le Grotte d'Italia* **IV**(4): 1–46.

Pasini G. 1973. Sull'importanza speleogenetica dell'«Erosione antigravitativa*Le Grotte d'Italia* **IV**(4): 297–308.

Pasini G. 2009. A terminological matter: paragenesis, antigravitative erosion or antigravitational erosion? *International Journal of Speleology* **38**(2): 129–128.

Pasini G. 2012. Speleogenesis of the 'Buco dei Vichi' inactive swallow hole (Monte Croara karst sub-area, Bologna, Italy), an outstanding example of antigravitative erosio (or 'paragenesis' in selenitic gypsum. An outline of the 'post-antigravitative erosion'*Acta Carsologica* **41**(1): 15–34.

Piccini L. 2011. Speleogenesis in highly geodynamic contexts: the quaternary evolution of Monte Corchia multi-level karst system (Alpi Apuane, Italy). *Geomorphology* **134**(1–2): 49–61.

Piccini L, De Waele J, Galli E, Polyak VJ, Bernasconi SM, Asmerom Y. 2015. Sulphuric acid speleogenesis and landscape evolution: Montecchio cave, Albegna river valley (Southern Tuscany, Italy). *Geomorphology* **229**: 134–143.

Picotti V, Pazzaglia FJ. 2008. A new active tectonic model for the construction of the Northern Apennines mountain front near Bologna (Italy). *Journal of Geophysical Research* **113**: B08412.

Pisias NG, Moore T. 1981. The evolution of Pleistocene climate: a time series approach. *Earth and Planetary Science Letters* **52**(2): 450–458.

Plan L, Tschegg C, De Waele J, Spötl C. 2012. Corrosion morphology and cave wall alteration in an Alpine sulfuric acid cave (Kraushohle, Austria). *Geomorphology* **169**: 45–54.

Polyak VJ, McIntosh WC, Güven N, Provencio P. 1998. Age and origin of Carlsbad CAVERN AND RELATED CAVES from ^{40}Ar/^{39}Ar of Alunite. *Science* **279**(5358): 1919–1922.

Polyak VJ, Provencio P, Asmerom Y. 2016. U–Pb dating of speleogenetic dolomite: a new sulfuric acid speleogenesis chronometer. *International Journal of Speleology* **45**(2): 103–109.

Pons-Branchu E, Douville E, Roy-Barman M, Dumont E, Branchu P, Thil F, Frank N, Bordier L, Borst W. 2014. A geochemical perspective on Parisian urban history based on U-Th dating, laminae counting and yttrium and REE concentrations of recent carbonates in underground aqueducts. *Quaternary Geochronology* **24**: 44–53.

Roveri M, Flecker R, Krijgsman W, Lofi J, Lugli S, Manzi V, Sierro FJ, Bertini A, Camerlenghi A, De Lange G, Govers R, Hilgen FJ, Hübscher C, Meijer PT, Stoica M. 2014. The Messinian salinity crisis: past and future of a great challenge for marine sciences. *Marine Geology* **352**: 25–58.

Sasowsky ID. 1998. Determining the age of what is not there. *Science* **279**(5358): 1874.

Scroxton N, Gagan MK, Dunbar GB, Ayliffe LK, Hantoro WS, Shen C-C, Hellstrom JC, Zhao J-X, Cheng H, Edwards RL, Sun H, Rifai H. 2016. Natural attrition and growth frequency variations of stalagmites in southwest Sulawesi over the past 530 000 years. *Palaeogeography Palaeoclimatology Palaeoecology* **441**: 823–833.

Simoni A, Ponza A, Picotti V, Berti M, Dinelli E. 2013. Earthflow sediment production and holocene sediment record in a large Apennine catchment. *Geomorphology* **188**: 42–53.

Sirocko F, Claussen M, Sánchez Goñi MF, Litt T. 2006. The climate of past interglacials. *Developments in Quaternary Science* **7**: 622.

Spötl C, Mattey D. 2012. Scientific drilling of speleothems – a technical note. *International Journal of Speleology* **41**(1): 29–34.

Tassy A, Mocochain L, Bellier O, Braucher R, Gattacceca J, Bourlès D. 2013. Coupling cosmogenic dating and magnetostratigraphy to constrain the chronological evolution of peri-Mediterranean karsts during the Messinian and the Pliocene: example of Ardèche Valley, Southern France. *Geomorphology* **189**: 81–92.

Tzedakis PC, Raynaud D, McManus JF, Berger A, Brovkin V, Kiefer T. 2009. Interglacial diversity. *Nature Geoscience* **2**(11): 751–755.

Vai GB, Martini IP. 2001. *Anatomy of an Orogen: the Apennines and Adjacent Mediterranean*. Kluwer Academic Publishers, Dordrecht, Netherlands, 631.

Wegmann KW, Pazzaglia FJ. 2009. Late Quaternary fluvial terraces of the Romagna and Marche Apennines, Italy: climatic, lithologic, and tectonic controls on terrace genesis in an active orogen. *Quaternary Science Reviews* **28**(1): 137–165.

White WB. 1988. *Geomorphology and Hydrology of Karst Terrains*. Oxford University Press, New York, 464.

Williams PW. 1982. Speleothem dates, quaternary terraces and uplift rates in New Zealand. *Nature* **298**(5871): 257–260.

Woodhead J, Hellstrom J, Maas R, Drysdale R, Zanchetta G, Devine P, Taylor E. 2006. U-Pb geochronology of speleothems by MC–ICPMS. *Quaternary Geochronology* **1**(3): 208–221.

